Stem Cell Research (2013) 11, 902–912

Available online at www.sciencedirect.com

SciVerse ScienceDirect

www.elsevier.com/locate/scr

Polysome profiling shows extensive posttranscriptional regulation during human adipocyte stem cell differentiation into adipocytes

Lucia Spangenberg[b,1], Patricia Shigunov[a,1], Ana Paula R. Abud[a], Axel R. Cofré[a], Marco A. Stimamiglio[a], Crisciele Kuligovski[a], Jaiesa Zych[a], Andressa V. Schittini[a], Alexandre Dias Tavares Costa[a], Carmen K. Rebelatto[c], Paulo R.S. Brofman[c], Samuel Goldenberg[a], Alejandro Correa[a], Hugo Naya[b], Bruno Dallagiovanna[a,*]

[a] *Instituto Carlos Chagas, Fiocruz-Paraná, Rua Professor Algacyr Munhoz Mader, 3775, Curitiba-PR 81350-010, Brazil*
[b] *Unidad de Bioinformática, Institut Pasteur Montevideo, Mataojo 2020, Montevideo 11400, Uruguay*
[c] *Núcleo de Tecnologia Celular, Pontifícia Universidade Católica do Paraná, Rua Imaculada Conceição, 1155, Curitiba-PR 80215-901, Brazil*

Received 22 December 2012; received in revised form 29 May 2013; accepted 2 June 2013
Available online 10 June 2013

Abstract Adipocyte stem cells (hASCs) can proliferate and self-renew and, due to their multipotent nature, they can differentiate into several tissue-specific lineages, making them ideal candidates for use in cell therapy. Most attempts to determine the mRNA profile of self-renewing or differentiating stem cells have made use of total RNA for gene expression analysis. Several lines of evidence suggest that self-renewal and differentiation are also dependent on the control of protein synthesis by posttranscriptional mechanisms. We used adipogenic differentiation as a model, to investigate the extent to which posttranscriptional regulation controlled gene expression in hASCs. We focused on the initial steps of differentiation and isolated both the total mRNA fraction and the subpopulation of mRNAs associated with translating ribosomes. We observed that adipogenesis is committed in the first days of induction and three days appears as the minimum time of induction necessary for efficient differentiation. RNA-seq analysis showed that a significant percentage of regulated mRNAs were posttranscriptionally controlled. Part of this regulation involves massive changes in transcript untranslated regions (UTR) length, with differential extension/reduction of the 3′UTR after induction. A slight correlation can be observed between the expression levels of differentially expressed genes and the 3′UTR length. When we considered association to polysomes, this correlation values increased. Changes in the half lives were related to the extension of the 3′UTR, with longer UTRs mainly stabilizing the transcripts. Thus, changes in the length of these extensions may be associated with changes in the ability to associate with polysomes or in half-life.

* Corresponding author. Fax: +55 41 33163267.
E-mail address: brunod@tecpar.br (B. Dallagiovanna).
[1] Both authors contributed equally to this work.

1873-5061/$ - see front matter © 2013 Elsevier B.V. All rights reserved.
http://dx.doi.org/10.1016/j.scr.2013.06.002

Introduction

Human adipose tissue-derived stromal cells (hASC) are readily isolated from the pools of cells resident in the vascular stroma of adipose tissue. ASCs proliferate and self-renew and, due to their multipotent nature, they can differentiate at least in vitro into several tissue-specific lineages, including the chondrogenic, osteogenic, adipogenic and miogenic lineages (De Ugarte et al., 2003; Gimble et al., 2007). Adipose tissue is ubiquitous and large quantities are easily accessible with minimal invasion procedures (Baer and Geiger, 2012). These characteristics make these cells ideal candidates for use in cell therapy. An understanding of the biological process committing the cell to differentiation into a specific cell type is essential for the successful repair of injured tissue.

Cytokines, growth factors and extracellular matrix components in the microenvironment determine stem cell fate, by regulating the switch from self-renewal to differentiation (Kratchmarova et al., 2005). However, the downstream effectors and the gene regulatory networks controlling these processes remain unclear. Gene expression profiling has provided insight into the molecular pathways involved in ASC self-renewal and differentiation (Ivanova et al., 2002; Song et al., 2006). Genome-wide analyses based on microarray hybridization and, more recently, next generation sequencing, have been carried out to assess the global expression of gene networks.

Most attempts to determine the mRNA profile of self-renewing or differentiating cells have made use of total RNA for hybridization to microarrays or RNA-Seq analysis (Jeong et al., 2007a; Menssen et al., 2011). High-throughput analyses in eukaryotes comparing mRNA and protein levels have indicated that there is no direct correlation between transcript levels and protein synthesis, suggesting a high degree of posttranscriptional regulation in eukaryote cells (Washburn et al., 2003; Keene, 2007; Tebaldi et al., 2012). This hampers the classical transcriptome-based approach to investigate controlled expression in differentiating cells. Protein abundance can be controlled and refined through the regulation of gene expression at various complementary levels. Several lines of evidence from different organisms suggest that stem cell self-renewal and differentiation are also dependent on the control of protein synthesis by posttranscriptional mechanisms (Keene, 2007; Sampath et al., 2008; Haston et al., 2009; Kolle et al., 2011). The analysis of the mRNA fraction associated to polysomes has been used as a strategy to analyze posttranscriptional mechanisms involved in the control of translation (Fromm-Dornieden et al., 2012). This posttranscriptional regulation is mediated by various molecules, such as microRNAs, noncoding RNAs and RNA binding proteins. *Trans*-acting factors recognize and bind sequences or structural elements, mostly in the untranslated regions (UTRs) of mRNAs (Mittal et al., 2009; Bar et al., 2008; Keene, 2010). Posttranscriptional control may be mediated by, amongst other things, modifications to mRNA stability or by the inhibition of transcript association with translating ribosomes.

We used adipogenic differentiation as a model, to investigate the extent to which posttranscriptional regulation controlled gene expression in hASCs. We focused on the initial steps of cell differentiation and isolated both the total mRNA fraction and the subpopulation of mRNAs associated with translating ribosomes. RNA-seq analysis showed that a significant percentage of regulated mRNAs were controlled both at the translational level and by changes to their half lives. Part of this regulation is associated with differential extension/reduction of the 3′UTR after induction.

Materials and methods

Isolation, culture, and differentiation of hASCs

Stem cells were obtained from adipose tissue from obese human donors (two males and one female, ages: 41, 52, 23). All samples were isolated, collected after informed consent had been obtained, in accordance with guidelines for research involving human subjects, and with the approval of the Ethics Committee of Fundação Oswaldo Cruz, Brazil (approval number 419/07). hASCs were isolated, cultured and characterized as previously described (Rebelatto et al., 2008). Briefly, 100 ml of adipose tissue was washed with sterile phosphate-buffered saline (PBS) (Gibco Invitrogen). A one-step digestion by 1 mg/ml collagenase type I (Invitrogen) was performed for 30 min at 37 °C during permanent shaking and was followed by filtration through first a 100- and then 40-μm mesh filter (BD FALCON, BD Biosciences Discovery Labware, Bedford, MA, USA). The cell suspension was centrifuged at 800 *g* for 10 min, and contaminating erythrocytes were removed by erythrocyte lysis buffer, pH 7.3. The cells were washed and then cultivated at a density of 1×10^5 cells/cm^2 in T75 culture flasks in DMEM-F12 (Gibco Invitrogen) supplemented with 10% FCS, penicillin (100 units/ml), and streptomycin (100 μg/ml). The medium was changed 2 days after the initial plating. The culture medium was then replaced twice each week. ASCs were subcultured after the cultures had reached 80% to 90% confluence; cells were detached by treatment with 0.25% trypsin/EDTA (Invitrogen) and were replated as passage-1 cells (the process was then continued). The characterization of the cells has been done following the minimal criteria for defining multipotent mesenchymal stromal cells as determined by the International Society for Cellular Therapy (Dominici et al., 2006). All tests were performed with cell cultures at passages 3 to 5. For adipogenic differentiation, hASCs were treated with hMSC Adipogenic Differentiation Bullet Kit (Lonza), in accordance with the manufacturer's instructions. Briefly, adipogenic differentiation was induced by 6 day cycles of induction/maintenance during 21 days. Induction medium contained the adipogenic inducers insulin, dexamethasone, indomethacin and IBMX; maintenance medium contained insulin. The medium was changed every 3 days. The degree of adipogenic differentiation was determined by assessing the cytoplasmic accumulation of triglycerides by staining with Oil Red O or Nile Red (Sigma-Aldrich), as described by Rebelatto et al. (2008). We also performed reverse transcription-polymerase chain reaction (RT-PCR) to estimate the amount of adipocyte-specific fatty acid-binding protein 4 (FABP4) mRNA. A list of the primers used is provided in Supporting Information Table S1.

Sucrose density gradient separation and RNA purification

Polysomal fractions were prepared with a modified version of the procedure described by Holetz et al. (2007). In brief,

hASC cultures at 50 to 60% confluence were treated with 0.1 mg/ml cycloheximide (Sigma-Aldrich) for 10 min at 37 °C. The cells were removed from the culture flasks with a cell scraper and resuspended in 0.1 mg/ml cycloheximide in PBS. The suspension was centrifuged (2000 ×*g* for 5 min) and the resulting pellet was washed twice with 0.1 mg/ml cycloheximide in PBS. The cells were lysed by incubation for 10 min on ice with polysome buffer (15 mM Tris–HCl pH 7.4, 1% Triton X-100, 15 mM $MgCl_2$, 0.3 M NaCl, 0.1 μg/ml cycloheximide, 1 mg/ml heparin). The cell lysate was centrifuged at 12,000 ×*g* for 10 min at 4 °C. The supernatant was carefully isolated, loaded onto 10% to 50% sucrose gradients and centrifuged at 39,000 rpm (SW40 rotor, HIMAC CP80WX HITACHI) for 160 min at 4 °C. The sucrose gradient was fractionated with the ISCO gradient fractionation system (ISCO Model 160 gradient former), connected to a UV detector for the monitoring of absorbance at 275 nm, and the polysome profile was recorded. The total and polysomal RNA fractions were extracted by a standard Trizol (Invitrogen) RNA isolation protocol.

cDNA library construction and RNA sequencing (RNA-Seq)

We subjected total and polysome-associated RNA samples to amplification with the Amino Allyl Message Amp II aRNA Amplification Kit (Ambion), to provide a template for SOLiD libraries. The cDNA libraries were prepared with the SOLiD Whole Transcriptome Analysis Kit and the purified products were evaluated with an Agilent Bioanalyzer (Agilent). Library molecules were subjected to clonal amplification according to the SOLiD Full-Scale Template Bead preparation protocol and sequenced with the SOLiD4 System (Applied Biosystems).

Data analysis

Quality control analysis was performed on the sequencing data, with NGSQC (Dai et al., 2010) software. Various quality parameters were explored visually for each sample (distribution of colors per sample/tile, genomic hit count per sample with different numbers of mismatches, sequencing read density and a quality score based on the mean values of the preceding values for each sample). All samples passed the quality control filter. Mapping and counting were performed with the R package Rsubread (Liao et al., 2013). Hierarchical clustering of the samples (log of counts plus one) was performed, to evaluate biological variability. Each sample was normalized to one million reads to account for library size. We also conducted a correspondence analysis (COA), a dimension reduction method, to the matrix of counts, to explore associations between variables. In COA it is possible to visualize samples and genes simultaneously, revealing associations between them. Genes, or samples, lying close to each other tend to behave similarly.

For the comparison of induced stem cells with undifferentiated stem cells we retained only those genes with counts of more than 1 per million in at least three conditions. In comparisons between induced stem cells and undifferentiated cells differentially expressed (DE) genes were identified with the edgeR bioconductor package (Robinson et al., 2010). This set of genes was used for GO term analysis with the goseq bioconductor package (Young et al., 2010).

The analysis of 3′UTR extension/shortening was performed according to the approach presented by Kolle et al. (2011), basically a sliding window of length w starting from last exon runs through the 3′UTR region (in steps of length s), each time determining expression of the window. If expression decays more than 50% the sliding stops and the 3′UTR ends. The parameters used in this case: w = 100 and s = 50. The analysis was restricted to the DE genes. A comparative analysis with proteomic data was performed against the murine data set of Molina et al. (2009). They have studied the proteomics of adipocyte differentiation on 3T3–L1 murine preadipocytes in four different time points (days 1, 3, 5 and 7) and determined differentially expressed genes on two sets of proteins, nuclear and secreted ones. The protein levels of both sets of genes were compared with the respective logFC determined by our differential expression analysis (in both cases polysomal and total RNA). Pearson correlation test was performed and significant results with the secreted protein set were obtained. Raw data has been submitted to the ArrayExpress repository under accession number E-MTAB-1366.

RT-qPCR

RT-PCR and real-time quantitative PCR (qPCR) were performed as previously described (Rebelatto et al., 2008). Glyceraldehyde-3-phosphate dehydrogenase (GAPDH) transcript was used as internal control. Experiments were performed with cells from at least three donors, with technical triplicates. Student's *t*-test was used to assess the significance of differences between the cell populations. We considered *p*-values < 0.05 to be statistically significant.

Reduced glutathione (GSH) determination

Cells were washed twice in PBS and centrifuged at low speed. Pelleted cells were suspended in lysis buffer (15 mM Tris–HCl, 15 mM $MgCl_2$, 300 mM NaCl, 1% Triton X-100; pH 7.4) and placed on ice for 10 min. Cell lysate was centrifuged at 12,000 ×*g* for 10 min and the supernatant was used to determine the level of reduced GSH. An aliquot (150 μl) of the supernatant was added to the reaction medium (25 μl of 3 mM DTNB [5,5′-dithiobis-(2-nitrobenzoic acid)] plus 125 μl of methanol) and absorbance was determined at 412 nm on a microplate reader (BioTek®). We calculated the concentration of reduced GSH, using the molar extinction coefficient of DTNB in solution (ε = 13,600 M^{-1} cm^{-1}). Results are expressed in μM GSH per 5 × 10^5 cells. All results are expressed as means ± SEM. The significance of the differences observed was evaluated by ANOVA, with Tukey's post hoc test. $p < 0.01$ and $p < 0.05$ were considered statistically significant. Raw data is shown in the Supplemental material Dataset S3.

Estimation of mRNA decay rates

For the measurement of mRNA stability, transcription was blocked by adding actinomycin D (Sigma) to the medium at a concentration of 10 mg/ml. The mean relative transcript levels estimated by RT-qPCR at each time point after the addition of Act D were used to estimate the half-life of the

transcript from a first-order decay model, according to the equation, $\gamma = \beta_0 e^{\beta t}_1 + \varepsilon$, where γ is the mean relative amount of mRNA at time t after the addition of Act D, β_0 is the initial quantity, β_1 is a decay parameter related to half-life ($t1/2 = \pm \ln 2 / \beta_1$) and ε is an error term (Sharova et al., 2009).

Results

Adipogenesis is committed in the first days of induction

We characterized the patterns of gene expression involved in the initial steps of adipogenesis. All accepted protocols use at least three days of strong induction to promote differentiation into adipocytes so we allowed hASCs to differentiate in vitro in the presence of adipogenic induction media for 72 h. All the experiments described were performed with at least three samples of hASCs from different donors, all used in early passages. After three days of in vitro differentiation, the cells displayed no clear change in phenotype or accumulation of lipids in the cytoplasm (Supporting information Figs. S1A, B). The cells were collected for isolation of total and polysomal RNA. The hASCs had a polysome profile typical of cells with low levels of translation activity, with low concentrations of polysome complexes present throughout the gradient. In the first few days of adipogenesis, the cells displayed no significant change in overall polysome profile (Supporting information Figs. S1C, D).

We isolated polysome-associated mRNAs from the gradient fractions corresponding to polysomes. The total and polysomal mRNA fractions of hASCs were analyzed by RNA-Seq, with the SOLiD4 system. In both cases, we compared time points 0 and 72 h after adipogenic induction. The total number of reads obtained for each sample is shown in Supporting information Table S2. The reads of all samples were mapped onto the reference genome (Hg19; NCBI Build 37.64), yielding a mean mapping percentage of approximately 54%. Hierarchical clustering shows that samples cluster first as a function of conditions (control, induced) and then by RNA fraction, rather than by donor, indicating that total and polysomal RNA populations are intrinsically more characteristic than donor "idiosyncrasy" (Fig. 1A). Correspondence Analysis (COA) produced similar results (Fig. 1B), with the first axis separating samples according to fraction and the second by conditions. Most transcripts were detected in both fractions (though with different levels of expression) while a significant number of transcripts were only present in one of the RNA populations. This could reflect the existence of regulatory mechanisms which modulate the efficiency of association with polysomes (Fig. 1C). We filtered out genes with very low counts, reducing the number of genes retrieved to just over 15,000 per comparison (see Array Express E-MTAB-1366 and Supporting information Table S2). Furthermore, we identified the differentially expressed (DE) genes using this reduced set

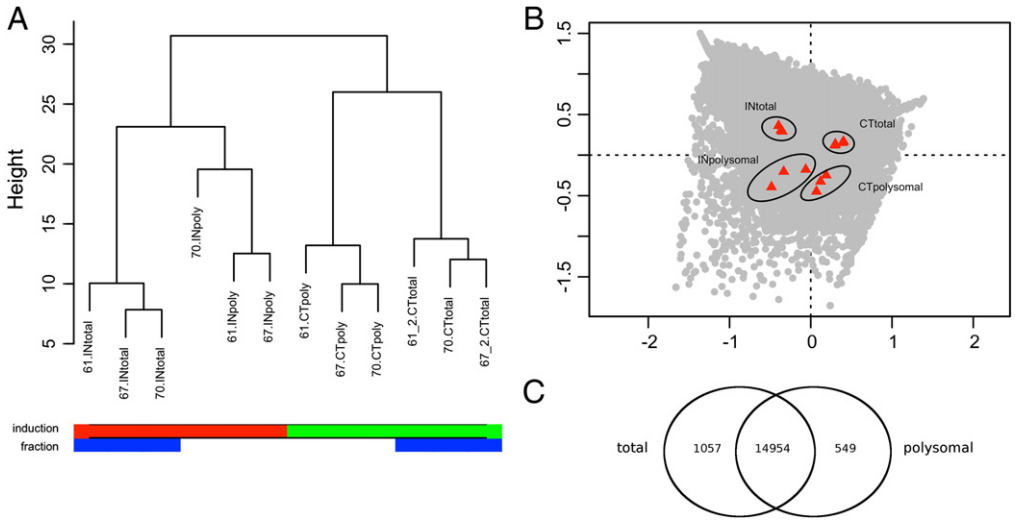

Figure 1 Results of hierarchical clustering and correspondence analysis showing the internal consistency of the data. (A): A dissimilarity based (bottom-up) hierarchical clustering was performed on the log-transformed counts of genes for the various samples. Initially, each object is assigned to its own cluster and then the algorithm proceeds iteratively, at each stage joining the two most similar clusters, according to some distance measure (in this case, complete linkage approach), continuing until there is one single cluster. The process is visualized as a dendrogram: the first branching event separates control (CT) from induced (IN) samples (IN left, CT right). Subsequent branching events group the samples according to the RNA fraction ("poly" and "total"). The numbers of the samples (61, 67 and 70) correspond to the donors. The height axis represents the distance between each branching event. Condition and fraction accounted for the largest proportions of the variance in both analyses, highlighting the consistency of the experiments. (B): Correspondence analysis (COA) on the samples. The x-axis represents the first component (the one explaining the most variance 43.43%) and the y-axis the second component (representing 29.91% of the variance). Fraction (polysomal and total) appears to be represented in the y-axis and the culture conditions (CT and IN) in the x-axis. Four groups of samples are represented on the reduced (two-dimensional) space. They correspond to the four RNA populations: CT-polysomal, CT-total, IN-polysomal, IN-total. (C): Venn diagram showing the overlap between the genes detected in both conditions: polysomal and total RNA populations. 14,954 genes are common to both sets.

(edgeR, paired comparisons). We compared the control and induced states, for the polysomal RNA fraction and for total RNA. We identified 2918 DE genes in total RNA and 780 DE genes in the polysomal fraction (FDR 0.001; Supporting information Datasets S1 and S2). Gene expression values (logFC) of both RNA fractions show Spearman correlation value of 0.62 (Supporting information Fig. S2). The relative efficiency of association with polysomes was also determined in both control and induced cells (Supporting information Table S3).

Differential expression was confirmed by RT-qPCR on selected transcripts (Supporting information Fig. S3). To also confirm the differential association with polysomes we performed sucrose density fractionation of polysomes. The presence of the selected transcripts in the RNA populations present in polysomes, monosomes and ribosome-free pooled fractions was analyzed by RT-qPCR. Differential expression was associated with a shift in the association of mRNAs with the different ribosome fractions for almost all transcripts tested but one (Supporting information Fig. S4).

More detailed analysis of the DE genes in the polysomal fraction showed a strong upregulation of adipogenesis-related genes after three days of induction. Key transcriptional regulators of the onset of adipogenesis, such as PPARG, KLF15 and CEBPα, showed an increase of several fold in their transcript levels (Supporting information Dataset S2). We also detected the expression of lipid metabolism-related genes and genes of the insulin response network encoding growth factors, receptors and binding proteins. These results suggest that adipogenesis is already triggered in the first few days of induction. Standard protocols are based on continuous or alternate induction, with the medium changed every three days and differentiation allowed to occur for up to 21 days. We tested our hypothesis, by inducing the cells for only three days and then allowing them to complete differentiation without further induction. The cells differentiated fully, but their fitness differed from that of cells induced for a continuous period of 21 days, and this difference was not the same for all considered donors (Fig. 2A). This raised questions about the true minimum period of stimuli required for the commitment of the cells to differentiation. Induction kinetics showed that three days was the critical time for the induction of efficient adipogenesis, although some degree of differentiation was observed with shorter induction times (Supporting information Table S4).

We observed the upregulation mainly in the polysomal RNA fraction of several genes involved in glutathione homeostasis in the cell. It has been reported that GSH decrement results in enhanced C/EBPβ activation, which is a key event in the first phase of adipogenesis, resulting in the activation of downstream PPARγ and a more rapid acquirement of adipose phenotype in 3T3–L1 cells (Vigilanza et al., 2011). For the confirmation of these results, we measured GSH levels in both control and induced cells. We found that differentiating cells contained 30% less GSH than non-induced cells (Fig. 2B).

Polysome associated mRNAs show extensive posttranscriptional regulation

GO analysis was performed using DE genes on the polysomal and total fractions (Fig. 3). Most of the GO terms underrepresented in both fractions were involved in nucleic acid metabolism and nuclear functions (Supporting information Tables S5, S6 and S7).

We obtained 18 overrepresented GO terms (FDR 0.001) in the analysis of DE genes in the total fraction. Most of these terms are related to proteins from the extracellular space and plasma membrane, with functions involved in cell adhesion, cell signaling, receptor activity and extracellular matrix proteins.

We also obtained 18 overrepresented terms in the analysis of polysomal fraction samples. Some of the GO terms obtained were similar to those for the total fraction (e.g. receptor activity, Figs. 3A, B), whereas several others were specific to the polysomal samples (oxidoreductase activity, Fig. 3A). Furthermore, some terms for which changes in mRNA levels were observed in the total fraction (genes encoding ribosomal or actin cytoskeleton proteins) showed no difference when polysomal RNA fraction was analyzed. In particular, no difference in polysome association was observed for transcripts encoding proteins involved in the development of the nervous system and in cell differentiation, despite the increase in the

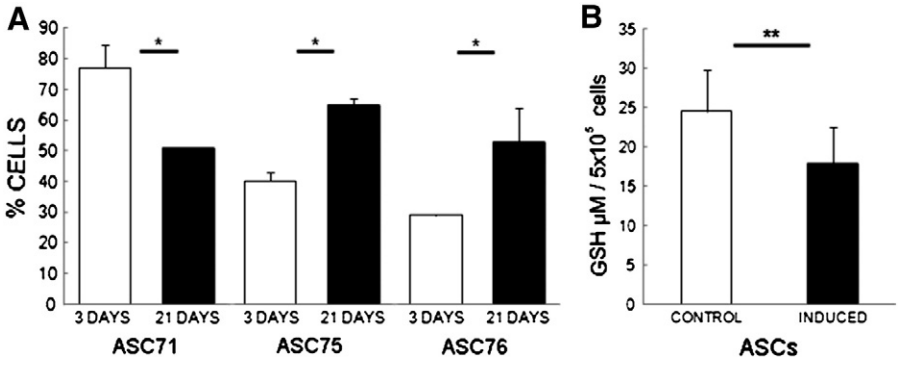

Figure 2 Morphological and metabolic changes during the differentiation process. (A): Differentiation potential analysis of ASCs: cells were maintained in differentiation-inducing conditions for 3 (white) or 21 days (black) and allowed to complete adipogenesis. Columns represent the percentage of differentiated cells in the cultures after 21 days. (B): Reduced glutathione (GSH) concentration in the induced cells (black column) was 30% lower than that in the control group (white column). The data shown are from three independent experiments carried out with ASCs from three donors. The results are expressed as means ± SD. The significance of differences between mean values was evaluated by a two-way analysis of variance (ANOVA) followed by a Tukey test. p values ≤ 0.01 and ≤ 0.05 were considered statistically significant.

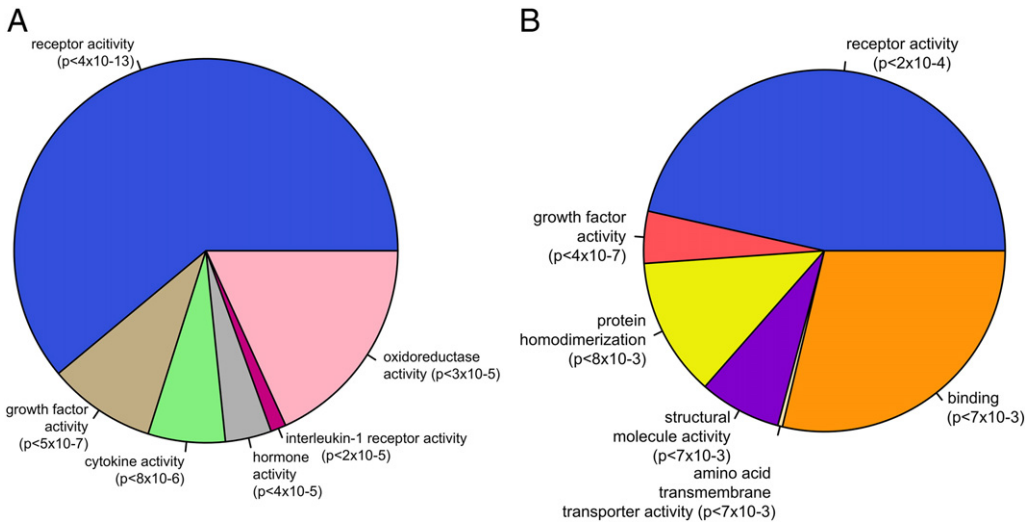

Figure 3 GO analysis of two sets of differentially expressed genes: IN vs CT in the polysomal RNA fraction (A) and IN vs CT in total RNA (B). Only overrepresented Molecular Function (MF) GO terms are shown in each pie chart in (A) and (B). For each over represented MF GO term its corresponding adjusted p-values are shown.

levels of transcripts for these proteins in the total fraction. To confirm our results we compared our data with previously published proteomic data. Proteomic analysis of human ASCs undergoing adipogenesis showed the differential expression of receptors and membrane proteins (Jeong et al., 2007b) and proteins related to oxido-reductase activity and oxidative stress response (Kim et al., 2010; Kheterpal et al., 2011). Moreover, we performed correlation analysis with the proteomic data of Molina et al. (2009) who presented a quantitative analysis (SILAC) of adipogenesis in murine 3T3–L1 cells. Molina's experiment determined protein expression levels during adipocyte differentiation at four time points (days 1, 3, 5 and 7) and for two sets of proteins: nuclear (280) and secreted (147) proteins. After determining the corresponding human orthologs we retrieved our logFC values of the comparison of IN wrt CT in the polysomal RNA fraction. No significant correlation was observed for the nuclear proteins set correlation values were not significant in each of the time points. This was expected as since we have observed a downregulation of nuclear proteins in our assays. However, the set of secreted proteins is highly correlated to our data for almost every time point and the correlation is also statistically significant (Supplementary information Fig. S5A). To further confirm our results, protein expression was also measured by western blot with protein extracts from control (CT) and induced (IN) cells. The amount of IGFBP2 protein was clearly increased in induced cells corroborating the differential expression of the insulin signaling pathway after induction. As mentioned previously, many transcripts that showed differential expression in the total fraction but not in their association with polysomes showed no changes when protein levels were analyzed (Supporting information Fig. S5B). These findings suggest that posttranscriptional mechanisms may have a key role in the control of gene expression during adipogenesis.

We compared differential expression between the total and polysomal RNA fractions, to assess the degree of posttranscriptional regulation, by an approach similar to that used by Lundberg et al. (2010). Using the differential expression values shown in Datasets S1 and S2, we compared the samples in the polysomal and total RNA fractions, using a cutoff value of $|\text{logFC}| > 1.5$. Fig. 4A shows logFC values obtained from the comparison of induced vs. control samples of the polysomal fraction against the logFC values obtained from the comparison of total RNA samples. Most of the genes identified displayed no change in expression level during differentiation (87.65%). However, 5.25% of the transcripts displayed changes in both RNA fractions, and another 5.45% of the transcripts displayed changes in steady-state RNA levels with no change in the amount of transcript associated with translating ribosomes. Finally, 1.66% of the transcripts displayed differential mobilization to the polysomes during cell differentiation. If restricted only to changing genes (in either fraction), almost half of the genes showed differential expression in both conditions (about 43%), about 13% were DE only in the polysomal fraction and about 44% were DE only in the total fraction (Fig. 4B). Our results demonstrate the existence of posttranscriptional mechanisms regulating the association of mRNAs with translating ribosomes, irrespectively of a change in steady-state levels. Hence, we observe an extensive posttranscriptional regulation during the initial steps of adipogenesis.

Cell differentiation involves massive changes in transcript UTR length

Recent studies have reported that the transcripts expressed in human and murine embryonic stem cells have alternative 3′UTRs (Kolle et al., 2011; Ji et al., 2009). It has been suggested that the 3′UTRs of mRNAs increase in length with the progression of embryonic development in mouse embryonic stem cells (Ji et al., 2009). We considered the reads mapped onto putative extended 3′UTR to detect possible changes during the induction of adipogenesis. We found that the differentially expressed genes displayed changes in the length of their 3′UTRs during this process. By contrast to the findings in mouse cells, we observed both lengthening and shortening of the 3′UTRs of these transcripts (Dataset S4).

The 3′UTRs of mRNAs potentially contain *cis*-acting elements for the posttranscriptional regulation of gene expression. Thus,

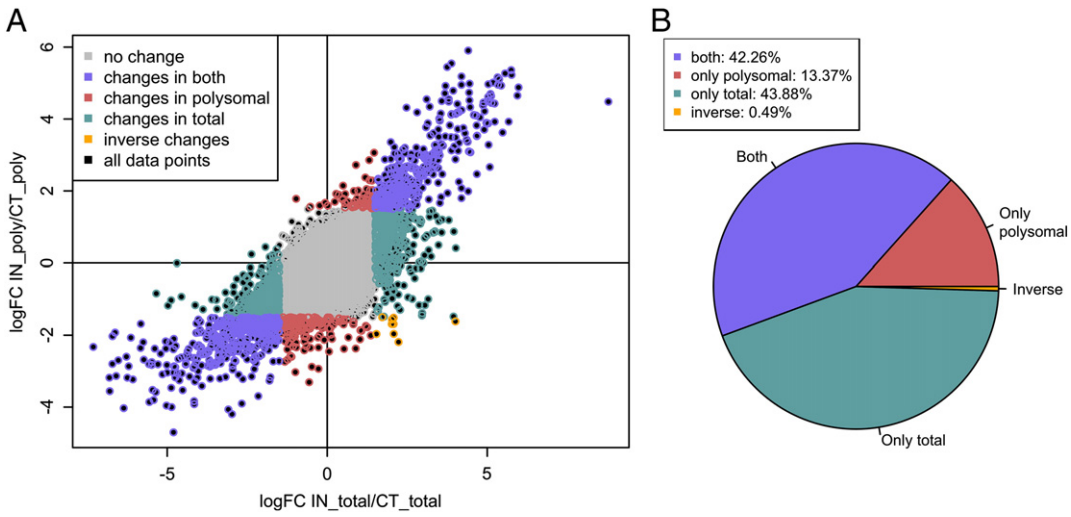

Figure 4 Differential association of mRNAs to polysomes: (A): LogFC values from different RNA fractions were compared. The logFC values (IN vs. CT) for the polysomal fraction (y-axis) were plotted against the logFC values for the total RNA fraction (x-axis). The data points are colored according to the change in the fractions. Genes displaying changes only in the polysomal fraction include genes with a |logFC| of at least 1.5 (|logFC| > 1.5) and genes with a |logFC| < 1.5 in the total fraction (light red). Changes in the total RNA fraction were associated with a |logFC| >1.5 and of |logFC| < 1.5 in the polysomal fraction (light green). Genes displaying changes in expression in both sets of conditions had high (or low) values of logFC (greater than 1.5/lower than −1.5) in both RNA fractions (violet). Inverse changes included genes with high logFC values (logFC > 1.5) in the total fraction and low values (logFC < 1.5) in the polysomal fraction, or vice versa (orange). (B): The pie chart on the right shows the percentages of genes displaying changes in expression in each of the four categories: change only in the polysomal fraction, change only in the total RNA fraction, concordant changes in the two fractions, discordant changes in the two fractions. Only the changing genes are considered.

changes in the length of these extensions may be associated with changes in the ability to associate with polysomes or in half-life. A slight correlation can be observed between the logFC of DE genes (total fraction) and the difference of 3′UTR length in control and induced samples. The correlation values are 0.28, 0.29, and 0.22 for donors 67, 61 and 70, respectively (Supporting information Table S8A). When we considered association to polysomes, these correlation values increase, 0.32, 0.35 and 0.25 respectively (Supporting information Table S8B). We also looked for a biological relationship between the different subsets of transcripts grouped by extension/shortening of the UTR and up or downregulation. Interestingly, we observed that the subset of downregulated transcripts presenting a longer 3′UTR after induction was related to the response to unfolded proteins and stress (Supplementary information Table S9).

We investigated the relationship between changes in UTR length and mRNA stability, by measuring the steady-state levels of the transcripts in control and induced cells. We focused on two examples, one extension (FABP4) and one shortening (WNT2) of transcript 3′UTRs which are differentiation markers or regulators of adipogenesis (Figs. 5A,D). Treatment of the cells with actinomycin D revealed changes in the half lives of these transcripts, which were directly related to the extension of the UTR in the two situations analyzed, with longer UTRs stabilizing the transcripts (Figs. 5 and S6). The results are summarized in Supporting information Table S10.

Discussion

Posttranscriptional regulation mechanisms are now considered to play a key role in the control of gene expression. Regulation occurs mainly through the modulation of mRNA half life or the formation of a translational initiation complex, allowing the assembly of translating polysomes (Keene, 2007).

We used adipogenesis as a cell differentiation model to study the regulation of gene expression in hASCs. The identification of mRNAs associated with polysomes could provide us with a clearer idea of which genes are actually translated into proteins in differentiating cells. By deep sequencing, we showed that adipogenesis had been triggered at the molecular level after three days of induction, although the cells did not yet display any clear phenotypic changes. Analysis of polysome associated mRNAs in the first hours of differentiation of 3T3 pre-adipocytes showed the upregulation of a discrete number of genes, mainly related with the overall control of translation (Fromm-Dornieden et al., 2012). We demonstrated, after three days of adipogenic induction, an upregulation of the expression of networks of genes involved in adipocyte differentiation (Menssen et al., 2011). Three days was identified as the minimum induction time required for the initiation of adipogenesis, as shorter induction times resulted in lower percentages of mature adipocytes. Moreover, no additional induction was required to achieve differentiation, suggesting that the cells can sustain their own differentiation, once committed. Differentiating hASCs contain high levels of expression of prolactin (PRL) (See Dataset S2). Studies with murine preadipocytes have demonstrated that fetal bovine serum (FBS), which is known to contain large amounts of prolactin (Ginsburg and Vonderhaar, 1995), is required for the efficient induction of adipogenesis and that PRL can replace FBS in the differentiation of the 3T3–L1 preadipocyte cell line (Stewart et al., 2004). PRL has also been shown to act as an adipogenesis-enhancing hormone,

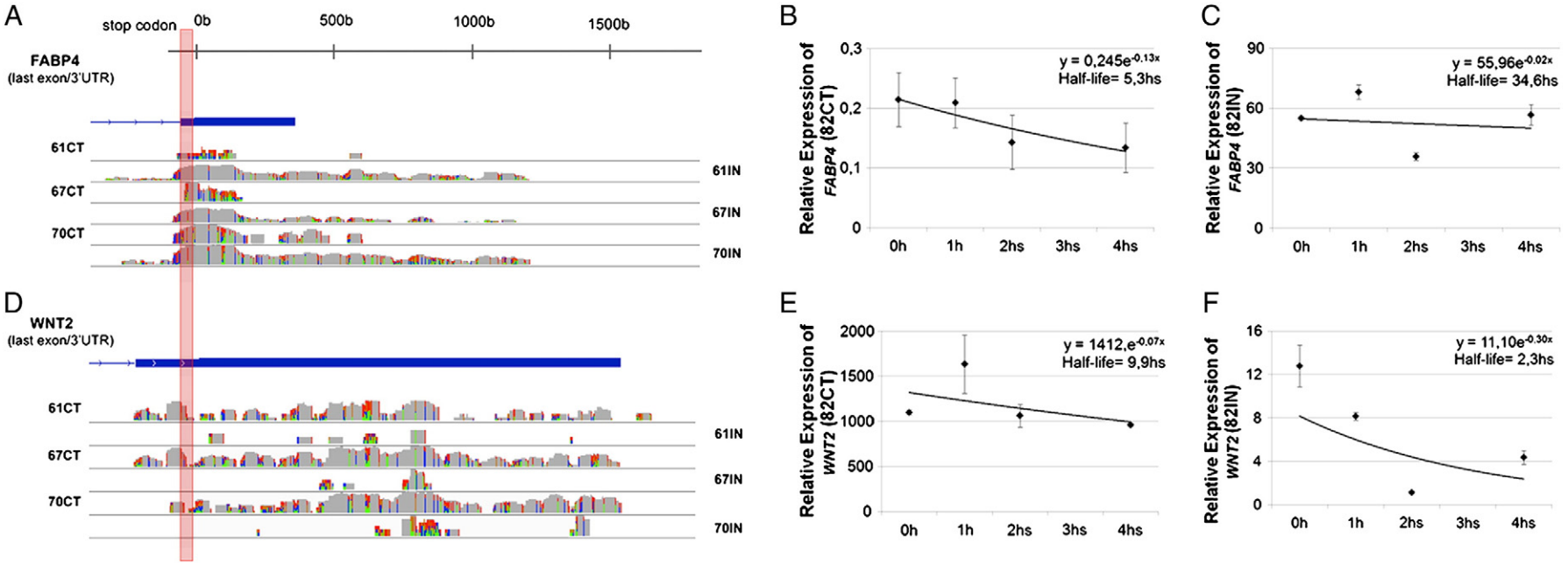

Figure 5 The coverage vectors of the 3′UTR of two genes and the half-life of the mRNA. (A): Six samples (3 CT and 3 IN) are represented as coverage vectors (log-scaled) for the *FABP4* gene. Only experiments using polysomal RNA were considered. The induced and control samples are interspersed (e.g. 61 CT and 61 IN). Induced samples of show an extension the 3′UTR (~1 kb). The red vertical bar shows the stop codon, the horizontal blue bars represent the last portion of the gene structure (last exon and 3′UTRs). (D): Same analysis for the *WNT2* gene. In this case, induced samples show a shortening of the 3′UTR, whereas control samples have a longer 3′UTR. (B–C, E–F): Half-life of *FABP4* and *WNT2* mRNAs in control (CT) and induced (IN) hASCs. hASCs were treated with Act-D for various periods, to block mRNA synthesis. Total RNA isolation, cDNA generation and real-time PCR amplification were performed as described in the text. The values shown are means ± SD of *FABP4* and *WNT2* RNA copy number per μg of total RNA, from two independent experiments carried out in triplicate.

enhancing the expression of the key transcriptional regulators of adipogenesis, C/EBPβ and PPARγ (Nanbu-Wakao et al., 2000). Interestingly, for bone marrow stromal cells, the induction of adipogenesis causes a dose-dependent increase in prolactin receptor expression, suggesting a role for prolactin and its receptor in adipocyte differentiation (McAveney et al., 1996). Studies in knockout mice have shown that an absence of PRL receptor (PRLR) signaling compromises the growth and differentiation of brown adipose tissue and that immortalized PRLR knockout preadipocytes do not differentiate into mature adipocytes, this defect being reversed by the reintroduction of PRLR (Viengchareun et al., 2008). Moreover, the production of PRL mRNA and protein increases markedly during the early differentiation of primary human preadipocytes (Hugo et al., 2006).

Clustering analysis of the total and polysomal RNA fractions showed these two fractions to be clearly different, regardless of donor origin. GO analysis revealed enrichment in different terms in the two populations. Nucleic acid metabolism-related genes were clearly downregulated in both fractions. As this category includes genes encoding regulatory proteins, further studies are required to understand the impact of this negative control on MSC differentiation. Genes encoding membrane-related and receptor proteins were upregulated in both RNA populations, suggesting that the principal changes in MSC biology during differentiation are related to the response to external stimuli and signaling.

A comparison of the total RNA and polysome-associated fractions provides a global estimate of the degree of posttranscriptional regulation, at least in terms of the control of translation initiation (Halbeisen and Gerber, 2009). Almost 60% of the differentially expressed genes showed some kind of posttranscriptional regulation. In most cases, this regulation counterbalances fluctuations in total RNA levels. Thus, transcripts increasing or decreasing in abundance in the cell are recruited to polysomes in equal amounts in differentiating cells. It was also observed a subset of transcripts that, although overexpressed in both fractions, showed a higher fold change in the polysomal RNA fraction. This has been described as a mechanism of homodirectional co-regulatory mechanism resulting in the amplification or potentiation of the positive control of gene expression (Preiss et al., 2003). However, there is a subpopulation of mRNAs that is regulated solely at the translational level.

Specific groups of related genes were found to display differential expression mostly in the polysomal fraction. In particular, oxidative stress response genes and a family of genes encoding proteins involved in the response to changes in the levels of reduced glutathione (GSH), such as glutathione peroxidases (GPxs) (Brigelius-Flohe, 1999), aldo-keto reductases (Barski et al., 2008) and metallotioneins (Nielsen et al., 2007), displayed expression patterns of this type. Oxidative stress may occur as a result of adipogenic differentiation or lipid metabolism, and the upregulation of these genes may contribute to a protective response. GPxs are involved in various reactions, such as the reduction of organic hydroperoxides (ROOH) by GSH conjugation (Arteel and Sies, 2001). We found that the concentration of reduced glutathione (GSH) was 30% lower in induced than in control cells. This higher level of activity of enzymes involved in GSH homeostasis may counteract the higher ROS concentrations in differentiated cells (Yang et al., 2012).

Posttranscriptional regulation is usually mediated by the interaction of *trans*-acting factors with the UTR regions. Thus, 3′UTRs appear to play a key role in posttranscriptional regulation, as the spatial platform bearing the sequence or structural elements in *cis* that are targeted by regulatory factors (Mignone et al., 2002). Specific modulations of UTR length in tissues have been reported, based on either the use of different polyadenylation signals or alternative splicing (Zhang et al., 2005). The length of 3′UTRs has been shown to differ between embryonic stem cells and somatic cells, in both humans and mice. In human embryonic stem cells, some transcripts have 3′UTRs several kilobases longer than the reported length (Kolle et al., 2011). Proliferating cells produce mRNAs with shorter UTRs, which have longer half-lives. It has been suggested that transcripts may be stabilized by the loss of miRNA binding sites, which usually downregulate gene expression (Sandberg et al., 2008). By contrast, in murine stem cells, the UTRs of tissue-specific transcripts increase in length following cell commitment. This extension results from the use of distal polyadenylation sites and results in an increase in the half life of the mRNA, by an unknown mechanism (Ji et al., 2009). Moreover, in brown and white adipose tissues, Ptitsyn and Gimble (2007) reported the existence of oscillatory patterns of expression of SOCS3 and JAK transcripts. Shorter and longer transcripts oscillate in opposite phases. These transcripts were generated by alternative polyadenylation in response to circadian rhythms. The relationship between alternative polyadenylation, circadian rhythms and posttranscriptional regulation mechanisms like mRNA decay needs to be determined. Nocturnin, a circadian deadenylase, enhances adipogenesis via interaction with PPAR-γ and could be a possible link between these mechanisms (Green et al., 2007; Kawai et al., 2010). However, we didn't detect Nocturnin among the DE genes which are in accordance with previous results showing that Nocturnin is not upregulated by insulin induction in bone-marrow stem cells (Kawai et al., 2010). We observed a shortening of some 3′UTRs and an extension of others following the induction of cell differentiation. Even though we recognize the limitations of our approach to estimate the actual length of the 3′UTR (biased wrt gene expression, no estimation of sampling "holes", arbitrary parameters) we obtain a first overview of the situation; many 3′UTRs are changing sizes, in both directions (extension/shortening). We found some hints supporting that the length of the UTR is directly related to the stability of the mRNA and to enhanced association to polysomes. As reported for mouse stem cells, we found a bias towards longer 3′UTRs resulting in more stable transcripts though this is not a general rule. A preliminary analysis of the alternative UTRs strongly suggests that they resulted from differential polyadenylation. Epigenetic mechanisms as histone acetylation could be involved in the choice or selection for alternative polyadenylation sites resulting in new 3′UTRs that could also regulate transcription. In 3T3 preadipocytes the 3′UTR of C/EBPβ acts as a strong enhancer element as a result of differential histone acetylation (Zhang et al., 2012). In chondrocytes, the 3′UTR of the Col2A1 gene is also a potent enhancer factor. It interacts with the promoter region through gene looping resulting in upregulation of gene expression (Jash et al., 2012). The mechanisms involved in the selection of alternative polyadenylation sites remain to be identified. It seems likely that extension of the 3′UTRs results in the

presence of new and additional regulatory elements, both positive and negative in effect.

Conclusions

Our results show that extensive posttranscriptional regulation occurs during the adipogenic differentiation of hASCs. Analysis of polysome associated transcripts showed that adipogenesis is committed after three days of induction. Differentially expressed transcripts showed else shortening or extension of their 3′UTRs. This modification in the extension of the 3′UTRs could be associated to mechanisms acting on both RNA stability and translation. The coordination of different levels of regulation ensures the efficient and correct differentiation of stem cells, and an elucidation of these mechanisms is required for an adequate understanding of the determination of stem cell fate.

Supplementary data to this article can be found online at http://dx.doi.org/10.1016/j.scr.2013.06.002.

Acknowledgments

This work was supported by grants from *Ministério da Saúde* and *Conselho Nacional de Desenvolvimento Cientifico e Tecnológico* — CNPq, *FIOCRUZ-Pasteur Research Program* and *Fundação Araucária*. L.S. received fellowship from ANII (Agencia Nacional de Investigación e Innovación, Uruguay); S.G., J.Z. and B.D. from *CNPq*, P.S., A.C. and M.A.S. from *FIOCRUZ*.

References

Arteel, G.E., Sies, H., 2001. The biochemistry of selenium and the glutathione system. Environ. Toxicol. Pharmacol. 10, 153–158.

Baer, P.C., Geiger, H., 2012. Adipose-derived mesenchymal stromal/stem cells: tissue localization, characterization, and heterogeneity. Stem Cells Int. 2012, 812693.

Bar, M., Wyman, S.K., Fritz, B.R., Qi, J., Garg, K.S., Parkin, R.K., Kroh, E.M., Bendoraite, A., Mitchell, P.S., Nelson, A.M., Ruzzo, W.L., Ware, C., Radich, J.P., Gentleman, R., Ruohola-Baker, H., Tewari, M., 2008. MicroRNA discovery and profiling in human embryonic stem cells by deep sequencing of small RNA libraries. Stem Cells 26, 2496–2505.

Barski, O.A., Tipparaju, S.M., Bhatnagar, A., 2008. The aldo-keto reductase superfamily and its role in drug metabolism and detoxification. Drug Metab. Rev. 40, 553–624.

Brigelius-Flohe, R., 1999. Tissue-specific functions of individual glutathione peroxidases. Free Radic. Biol. Med. 27, 951–965.

Dai, M., Thompson, R.C., Maher, C., Contreras-Galindo, R., Kaplan, M.H., Markovitz, D.M., Omenn, G., Meng, F., 2010. NGSQC: cross-platform quality analysis pipeline for deep sequencing data. BMC Genomics 11 (Suppl. 4), S7.

De Ugarte, D.A., Morizono, K., Elbarbary, A., Alfonso, Z., Zuk, P.A., Zhu, M., Dragoo, J.L., Ashjian, P., Thomas, B., Benhaim, P., Chen, I., Fraser, J., Hedrick, M.H., 2003. Comparison of multi-lineage cells from human adipose tissue and bone marrow. Cells Tissues Organs 174, 101–109.

Dominici, M., Le Blanc, K., Mueller, I., Slaper-Cortenbach, I., Marini, F., Krause, D., Deans, R., Keating, A., Prockop, D., Horwitz, E., 2006. Minimal criteria for defining multipotent mesenchymal stromal cells. The International Society for Cellular Therapy position statement. Cytotherapy 8, 315–317.

Fromm-Dornieden, C., von der Heyde, S., Lytovchenko, O., Salinas-Riester, G., Brenig, B., Beissbarth, T., Baumgartner, B.G., 2012. Novel polysome messages and changes in translational activity appear after induction of adipogenesis in 3T3–L1 cells. BMC Mol. Biol. 13, 9.

Gimble, J.M., Katz, A.J., Bunnell, B.A., 2007. Adipose-derived stem cells for regenerative medicine. Circ. Res. 100, 1249–1260.

Ginsburg, E., Vonderhaar, B.K., 1995. Prolactin synthesis and secretion by human breast cancer cells. Cancer Res. 55, 2591–2595.

Green, C.B., Douris, N., Kojima, S., Strayer, C.A., Fogerty, J., Lourim, D., Keller, S.R., Besharse, J.C., 2007. Loss of Nocturnin, a circadian deadenylase, confers resistance to hepatic steatosis and diet-induced obesity. Proc. Natl. Acad. Sci. U. S. A. 104, 9888–9893.

Halbeisen, R.E., Gerber, A.P., 2009. Stress-dependent coordination of transcriptome and translatome in yeast. PLoS Biol. 7, e1000105.

Haston, K.M., Tung, J.Y., Reijo Pera, R.A., 2009. Dazl functions in maintenance of pluripotency and genetic and epigenetic programs of differentiation in mouse primordial germ cells in vivo and in vitro. PLoS One 4, e5654.

Holetz, F.B., Correa, A., Avila, A.R., Nakamura, C.V., Krieger, M.A., Goldenberg, S., 2007. Evidence of P-body-like structures in *Trypanosoma cruzi*. Biochem. Biophys. Res. Commun. 356, 1062–1067.

Hugo, E.R., Brandebourg, T.D., Comstock, C.E., Gersin, K.S., Sussman, J.J., Ben-Jonathan, N., 2006. LS14: a novel human adipocyte cell line that produces prolactin. Endocrinology 147, 306–313.

Ivanova, N.B., Dimos, J.T., Schaniel, C., Hackney, J.A., Moore, K.A., Lemischka, I.R., 2002. A stem cell molecular signature. Science 298, 601–604.

Jash, A., Yun, K., Sahoo, A., So, J.S., Im, S.H., 2012. Looping mediated interaction between the promoter and 3′ UTR regulates type II collagen expression in chondrocytes. PLoS One 7, e40828.

Jeong, J.A., Ko, K.M., Bae, S., Jeon, C.J., Koh, G.Y., Kim, H., 2007a. Genome-wide differential gene expression profiling of human bone marrow stromal cells. Stem Cells 25, 994–1002.

Jeong, J.A., Ko, K.M., Park, H.S., Lee, J., Jang, C., Jeon, C.J., Koh, G.Y., Kim, H., 2007b. Membrane proteomic analysis of human mesenchymal stromal cells during adipogenesis. Proteomics 7, 4181–4191.

Ji, Z., Lee, J.Y., Pan, Z., Jiang, B., Tian, B., 2009. Progressive lengthening of 3′ untranslated regions of mRNAs by alternative polyadenylation during mouse embryonic development. Proc. Natl. Acad. Sci. U. S. A. 106, 7028–7033.

Kawai, M., Green, C.B., Lecka-Czernik, B., Douris, N., Gilbert, M.R., Kojima, S., Ackert-Bicknell, C., Garg, N., Horowitz, M.C., Adamo, M.L., Clemmons, D.R., Rosen, C.J., 2010. A circadian-regulated gene, Nocturnin, promotes adipogenesis by stimulating PPAR-gamma nuclear translocation. Proc. Natl. Acad. Sci. U. S. A. 107, 10508–10513.

Keene, J.D., 2007. RNA regulons: coordination of post-transcriptional events. Nat. Rev. Genet. 8, 533–543.

Keene, J.D., 2010. The global dynamics of RNA stability orchestrates responses to cellular activation. BMC Biol. 8, 95.

Kheterpal, I., Ku, G., Coleman, L., Yu, G., Ptitsyn, A.A., Floyd, Z.E., Gimble, J.M., 2011. Proteome of human subcutaneous adipose tissue stromal vascular fraction cells versus mature adipocytes based on DIGE. J. Proteome Res. 10, 1519–1527.

Kim, J., Choi, Y.S., Lim, S., Yea, K., Yoon, J.H., Jun, D.J., Ha, S.H., Kim, J.W., Kim, J.H., Suh, P.G., Ryu, S.H., Lee, T.G., 2010. Comparative analysis of the secretory proteome of human adipose stromal vascular fraction cells during adipogenesis. Proteomics 10, 394–405.

Kolle, G., Shepherd, J.L., Gardiner, B., Kassahn, K.S., Cloonan, N., Wood, D.L., Nourbakhsh, E., Taylor, D.F., Wani, S., Chy, H.S., Zhou, Q., McKernan, K., Kuersten, S., Laslett, A.L., Grimmond,

S.M., 2011. Deep-transcriptome and ribonome sequencing redefines the molecular networks of pluripotency and the extracellular space in human embryonic stem cells. Genome Res. 21, 2014–2025.

Kratchmarova, I., Blagoev, B., Haack-Sorensen, M., Kassem, M., Mann, M., 2005. Mechanism of divergent growth factor effects in mesenchymal stem cell differentiation. Science 308, 1472–1477.

Liao, Y., Smith, G.K., Shi, W., 2013. The Subread aligner: fast, accurate and scalable read mapping by seed-and-vote. Nucleic Acids Res. 41 (10), e108.

Lundberg, E., Fagerberg, L., Klevebring, D., Matic, I., Geiger, T., Cox, J., Algenas, C., Lundeberg, J., Mann, M., Uhlen, M., 2010. Defining the transcriptome and proteome in three functionally different human cell lines. Mol. Syst. Biol. 6, 450.

McAveney, K.M., Gimble, J.M., Yu-Lee, L., 1996. Prolactin receptor expression during adipocyte differentiation of bone marrow stroma. Endocrinology 137, 5723–5726.

Menssen, A., Haupl, T., Sittinger, M., Delorme, B., Charbord, P., Ringe, J., 2011. Differential gene expression profiling of human bone marrow-derived mesenchymal stem cells during adipogenic development. BMC Genomics 12, 461.

Mignone, F., Gissi, C., Liuni, S., Pesole, G., 2002. Untranslated regions of mRNAs. Genome Biol. 3 (REVIEWS0004).

Mittal, N., Roy, N., Babu, M.M., Janga, S.C., 2009. Dissecting the expression dynamics of RNA-binding proteins in posttranscriptional regulatory networks. Proc. Natl. Acad. Sci. U. S. A. 106, 20300–20305.

Molina, H., Yang, Y., Ruch, T., Kim, J.W., Mortensen, P., Otto, T., Nalli, A., Tang, Q.Q., Lane, M.D., Chaerkady, R., Pandey, A., 2009. Temporal profiling of the adipocyte proteome during differentiation using a five-plex SILAC based strategy. J. Proteome Res. 8, 48–58.

Nanbu-Wakao, R., Fujitani, Y., Masuho, Y., Muramatu, M., Wakao, H., 2000. Prolactin enhances CCAAT enhancer-binding protein-beta (C/EBP beta) and peroxisome proliferator-activated receptor gamma (PPAR gamma) messenger RNA expression and stimulates adipogenic conversion of NIH-3 T3 cells. Mol. Endocrinol. 14, 307–316.

Nielsen, A.E., Bohr, A., Penkowa, M., 2007. The balance between life and death of cells: roles of metallothioneins. Biomark. Insights 1, 99–111.

Preiss, T., Baron-Benhamou, J., Ansorge, W., Hentze, M.W., 2003. Homodirectional changes in transcriptome composition and mRNA translation induced by rapamycin and heat shock. Nat. Struct. Biol. 10, 1039–1047.

Ptitsyn, A.A., Gimble, J.M., 2007. Analysis of circadian pattern reveals tissue-specific alternative transcription in leptin signaling pathway. BMC Bioinformatics 8 (Suppl. 7), S15.

Rebelatto, C.K., Aguiar, A.M., Moretao, M.P., Senegaglia, A.C., Hansen, P., Barchiki, F., Oliveira, J., Martins, J., Kuligovski, C., Mansur, F., Christofis, A., Amaral, V.F., Brofman, P.S., Goldenberg, S., Nakao, L.S., Correa, A., 2008. Dissimilar differentiation of mesenchymal stem cells from bone marrow, umbilical cord blood, and adipose tissue. Exp. Biol. Med. (Maywood) 233, 901–913.

Robinson, M.D., McCarthy, D.J., Smyth, G.K., 2010. edgeR: a bioconductor package for differential expression analysis of digital gene expression data. Bioinformatics 26, 139–140.

Sampath, P., Pritchard, D.K., Pabon, L., Reinecke, H., Schwartz, S.M., Morris, D.R., Murry, C.E., 2008. A hierarchical network controls protein translation during murine embryonic stem cell self-renewal and differentiation. Cell Stem Cell 2, 448–460.

Sandberg, R., Neilson, J.R., Sarma, A., Sharp, P.A., Burge, C.B., 2008. Proliferating cells express mRNAs with shortened 3′ untranslated regions and fewer microRNA target sites. Science 320, 1643–1647.

Sharova, L.V., Sharov, A.A., Nedorezov, T., Piao, Y., Shaik, N., Ko, M.S., 2009. Database for mRNA half-life of 19 977 genes obtained by DNA microarray analysis of pluripotent and differentiating mouse embryonic stem cells. DNA Res. 16, 45–58.

Song, L., Webb, N.E., Song, Y., Tuan, R.S., 2006. Identification and functional analysis of candidate genes regulating mesenchymal stem cell self-renewal and multipotency. Stem Cells 24, 1707–1718.

Stewart, W.C., Baugh Jr., J.E., Floyd, Z.E., Stephens, J.M., 2004. STAT 5 activators can replace the requirement of FBS in the adipogenesis of 3 T3-L1 cells. Biochem. Biophys. Res. Commun. 324, 355–359.

Tebaldi, T., Re, A., Viero, G., Pegoretti, I., Passerini, A., Blanzieri, E., Quattrone, A., 2012. Widespread uncoupling between transcriptome and translatome variations after a stimulus in mammalian cells. BMC Genomics 13, 220.

Viengchareun, S., Servel, N., Feve, B., Freemark, M., Lombes, M., Binart, N., 2008. Prolactin receptor signaling is essential for perinatal brown adipocyte function: a role for insulin-like growth factor-2. PLoS One 3, e1535.

Vigilanza, P., Aquilano, K., Baldelli, S., Rotilio, G., Ciriolo, M.R., 2011. Modulation of intracellular glutathione affects adipogenesis in 3T3–L1 cells. J. Cell. Physiol. 226, 2016–2024.

Washburn, M.P., Koller, A., Oshiro, G., Ulaszek, R.R., Plouffe, D., Deciu, C., Winzeler, E., Yates III, J.R., 2003. Protein pathway and complex clustering of correlated mRNA and protein expression analyses in *Saccharomyces cerevisiae*. Proc. Natl. Acad. Sci. U. S. A. 100, 3107–3112.

Yang, S.R., Rahman, I., Trosko, J.E., Kang, K.S., 2012. Oxidative stress-induced biomarkers for stem cell-based chemical screening. Prev. Med. 54, S42–S49 (Suppl.).

Young, M.D., Wakefield, M.J., Smyth, G.K., Oshlack, A., 2010. Gene ontology analysis for RNA-seq: accounting for selection bias. Genome Biol. 11, R14.

Zhang, H., Lee, J.Y., Tian, B., 2005. Biased alternative polyadenylation in human tissues. Genome Biol. 6, R100.

Zhang, Q., Ramlee, M.K., Brunmeir, R., Villanueva, C.J., Halperin, D., Xu, F., 2012. Dynamic and distinct histone modifications modulate the expression of key adipogenesis regulatory genes. Cell Cycle 11, 4310–4322.